



UNIVERSITÀ
DEGLI STUDI
FIRENZE

FLORE

Repository istituzionale dell'Università degli Studi di Firenze

SYMPLEX Experiment: first results on oceanic mesoscale dynamics and related primary production from AVHRR and SeaWIFS satellite

Questa è la Versione finale referata (Post print/Accepted manuscript) della seguente pubblicazione:

Original Citation:

SYMPLEX Experiment: first results on oceanic mesoscale dynamics and related primary production from AVHRR and SeaWIFS satellite data and field experiments / Bohm E.; B. Buongiorno Nardelli; C. Brunet; R. Casotti; F. Conversano; F. Corato; E. D'acunzo; F. D'ortenzio; D. Iudicone; L. Lazzara; O. Mangoni; M. Marcelli; S. Marullo; L. Massi; G. Mori; I. Nardello; C. Nuccio; M. Ribera d'Alcala; V. Saggiomo; R. Santoleri; M. Scardi; S. Sparnocchia; S. Tozzi; S. Zoffoli. - In: PROCEEDINGS - SPIE. - ISSN 1018-4732. - STAMPA. -

Availability:

This version is available at: 2158/393350 since: 2020-02-03T13:02:58Z

Publisher:

Society of Photo-Optical Instrumentation Engineers (SPIE)

Published version:

DOI: 10.1117/12.332717

Terms of use:

Open Access

La pubblicazione è resa disponibile sotto le norme e i termini della licenza di deposito, secondo quanto stabilito dalla Policy per l'accesso aperto dell'Università degli Studi di Firenze (<https://www.sba.unifi.it/upload/policy-oa-2016-1.pdf>)

Publisher copyright claim:

(Article begins on next page)

PROCEEDINGS OF SPIE
EUROPTO
SERIES

Earth Surface Remote Sensing II

Giovanna Cecchi
Eugenio Zilioli
Chairs/Editors

21, 24 September 1998
Barcelona, Spain

Sponsored by

CNR—National Research Council of Italy
NASA—National Aeronautics and Space Administration (USA)
EOS—The European Optical Society
The Commission of the European Communities, Directorate General
for Science, Research, and Development
SPIE—The International Society for Optical Engineering

Published by

SPIE—The International Society for Optical Engineering



Volume 3496

SPIE is an international technical society dedicated to advancing engineering and scientific applications of optical, photonic, imaging, electronic, and optoelectronic technologies.

SYMPLEX Experiment: first results on oceanic mesoscale dynamics and related primary production from AVHRR and SeaWiFS satellite data and field experiments.

Emanuele Böhm^d, Bruno Buongiorno Nardelli^a, Christophe Brunet^g, Raffaella Casotti^f, Fabio Conversano^f, Federico Corato^f, Emma D'Acunzo^d, Fabrizio D'Ortenzio^d, Daniele Iudicone^d, Luigi Lazzara^b, Olga Mangoni^f, Marco Marcelli^f, Salvatore Marullo^a, Luca Massi^b, Giovanna Mori^b, Ilaria Nardello^b, Caterina Nuccio^b, Maurizio Ribera d'Alcalá^f, Vincenzo Saggiomo^f, Rosalia Santoleri^d, Michele Scardi^f, Stefania Sparnocchia^e, Sasha Tozzi^f, Simona Zoffoli^d

^aCentro Ricerche Casaccia - ENEA - Roma

^bDipartimento di Biologia Vegetale, Università di Firenze - Firenze

^cDipartimento di Zoologia, Università Federico II - Napoli

^dIstituto di Fisica dell'Atmosfera - CNR - Roma

^eIstituto Talassografico di Trieste - CNR - Trieste

^fStazione Zoologica "A. Dohrn" - Napoli

^gUniversité Littorale - Wimereaux

1 INTRODUCTION

Upper ocean dynamics is characterised by a strong variability, at different scales, both in direction and structure of the flow. Mesoscale variability, which is ubiquitous in the world ocean, is often the dominant component in the variance spectrum of velocity¹ with relevant implications on water mass mixing and transformation and on the carbon transfer in the marine food web. Mesoscale activity is manifested through the formation of instabilities, meanders and eddies. Eddies generate either a doming of isopycnals (cyclones) or a central depression (anticyclones). This in turn modifies, among the others, nutrient and organism distributions in the photic zone eventually enhancing or depressing photosynthetic activity and other connected biological responses. The mechanism is similar to what has been thoroughly studied for the warm and cold core rings but at different spatial and temporal scales.

The enhancement of phytoplankton growth and the modification of photosynthetic parameters has been shown to occur *in situ* by means of a modulated fluorescence probe². More recently, an attempt to estimate the magnitude of this specific forcing on nutrient fluxes and primary production has also been conducted at different scales by modelling exercises^{3,4}, though with contrasting estimates the relative importance concerns. Because phytoplankton growth takes place when light, nutrients and cells are found at the same place, the increase in primary production favored by mesoscale eddies cannot be easily predicted. The incident light, the seasonality, the life-time of the structure, its intensity etc. can all influence the final yield. In addition, it has still to be determined which component of the community reacts faster and takes advantage of the new nutrients and how efficiently the new carbon is channeled in the food web. For what remote sensing is concerned, the detectability from the space of such structures is certainly dependent on the depth at which the upward distortion of isopycnals takes place. It can be supposed that a change in bio-optical signature of the whole structure could occur because of the 3-D dynamics of the eddy. If this holds true, then colour remote sensing coupled with sea level topography and sea surface temperature should be a powerful tool to track such transient structures.

The ALT-SYMPLEX program has been designed to better understand the relationship between short living eddies and carbon transfer in the food web. This is based on several experiments aimed to integrate remote sensing data (ocean colour and surface topography) and *in situ* data in order to evaluate the relationship between surface and sub-surface physical dynamics and its relations on chemical and biological aspects in presence of mesoscale features.

Here, we present the results of a synthetic preliminary analysis of the data collected during the three cruises conducted in the Sicily Channel. During the surveys hydrographic, acoustic current-meter, bio-optical and strictly biological data have been collected in coincidence with NOAA-14, SeaWiFS, ERS2 and Topex/Poseidon passes. These data, together with the full coverage of ERS, SeaWiFS and NOAA passes, will form the basis to describe the mesoscale dynamics of the studied area and its relation with the dynamics of primary production in the water column.

2 STUDY AREA

The channel of Sicily is an intermediate basin, connecting the western and the eastern Mediterranean Sea. Using a model for water exchanges and sea level adjustments, Garret⁵ stressed the importance of this channel in controlling the large scale circulation of the Mediterranean.

Many oceanographic surveys have been carried out in this area after the first investigations conducted by Saclant Centre for Marine Research, La Spezia in the seventies⁶. As a consequence, the general characteristics of currents are relatively well known. Especially for the western side of the channel, called strait of Sicily, various authors have estimated the fluxes and the temporal and spatial variability of the water masses^{6,7,8,9}. To date no definitive results have been obtained because of the number of phenomena occurring at different space and time scales and of the complex bottom topography in that area.

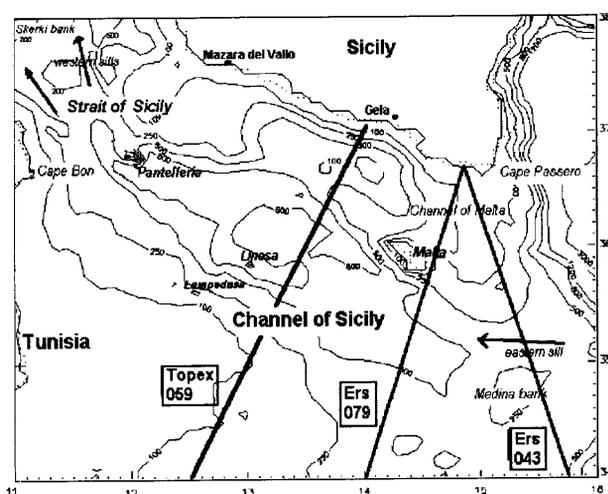


Fig.1 Bottom topography of the channel of Sicily

The channel of Sicily has a trapezoidal shape. The western side is 150 km wide with a mean depth of approximately 200 m. Two narrow sills of 430 m and 365 m make up the only deep connections to the western basin. The eastern side is much wider, extending for more than 500 km, but its mean depth does not exceed 200-300 m, except for the passage between Medina Bank and the island of Malta (eastern sill, 560 m, figure 1).

The channel is substantially a two-layer system. The fresher water of Atlantic origin (Modified Atlantic Water, MAW in the following) lies in the upper layer while the more saline Levantine Intermediate Water (LIW in the following) occupies the lower one (e.g.¹⁰). These two waters are separated by an intermediate transition layer whose thickness is known to vary between 30 m during winter and 100 m in summer¹¹.

In winter the MAW is found in the area between the African coast and the cold and saline front present along the northern Sicilian shelf (e.g.¹⁰). At this time the MAW flow is highest and its core is located on the African side of the channel. As surface layers become more and more isothermal through winter cooling and mixing, the thermocline progressively disappears. At this point the MAW jet can not be easily located¹². Hydrographic data and satellite imagery let us still distinguish meanders, eddies and intrusions of warm and saline water from the south of Malta to the centre of the channel. These structures are subjected to strong temporal and spatial variability.

During spring, temperature and salinity increase again due to evaporation and surface heating. The density gradient perpendicular to the flow reduces, causing a decrease in the baroclinic pressure and consequently in the geostrophic transport.

During summer MAW is found beneath a thin layer of warm and salty water and is characterised by the presence of fresher parcels down to 50 m¹⁰. The Atlantic water flow is composed by energetic mesoscale disturbances superimposed to the main current. During this period of the year thermal fronts associated with upwelling phenomena along Sicily are particularly evident.

On the other hand, the measurements taken in the Sicily Strait to date do not show seasonal variability in LIW characteristics and indicate that this water mass occupies the whole basin beneath 200 m^{6,8}. LIW slow westward movement is poorly monitored, mainly because of the extension of the area to be observed⁷.

It is important to stress that the LIW T-S characteristics in the Eastern and Western Mediterranean basins are quite different; therefore modification of LIW must occur in the Channel of Sicily. The analysis of the measures made in the strait of Sicily indicates that LIW should modify also at the eastern end of the channel, but very few measurements are available for this area.

It is very difficult to have a precise measure of the transport of the different water masses throughout the basin, mainly because of the extension of the channel on both ends. To date, the estimates of the mass flux computed by various authors for the western section of the channel, present significant discrepancies^{13,9}.

As a first conclusion the evidence of strong modification of the water masses flowing through the channel, reinforces the role of the intense mesoscale activity observed by satellite imagery and calls for a significant vertical transport of salt and nutrients.

3 ALT/SYMPLEX EXPERIMENT

The hydrographic data analysed in this contribution are those collected during the joint ALT and SYMPLEX cruises: ALT-SYMPLEX 1 (from the 12th of April to the 13th of May 1996) ALT-SYMPLEX 2 (from the 20th of July to the 11th of August 1997) and ALT-SYMPLEX 3 (from the 27th of March to the 20th of April 1998) on board of R/V Urania in the Sicily channel.

The ALT experiment is part of a research project approved by ESA in the framework of the Announcement of Opportunity for ERS-1 and ERS-2. It has the objective of studying the relationship between altimetric sea surface signals and 3-D structures of the ocean. Similarly, the Synoptic Mesoscale Plankton Experiment (SYMPLEX) is part of the NASA SeaWiFS program, as organized through the Announcement of Opportunity for SeaWiFS. Its main goal is to study the relation between the surface fields visible by remote-sensing satellites and physical and biological internal sea dynamics.

The ALT/SYMPLEX surveys were designed in order to satisfy the main objectives of the two experiments. The measurement were carried out in the eastern part of the Sicily Channel, where an intense mesoscale variability associated with a cold filament-like structure is observed in altimetric, infrared and colour satellite imagery. Observational strategy was based on repeated sampling of mesoscale eddies at relatively high frequency (hours) or structures such as filaments, frontal instabilities etc. It is worth noting that the scale of the structures of this study is shorter than the scale of structures formed as instabilities of main currents, such as the Algerian current. The corresponding lifetime is thus smaller which makes biological response less deterministic, and probably weaker, and the observational effort greater, both for searching and monitoring.

Therefore, a set of hydrographic, dynamical, optical, chemical and biological data was collected to characterise this region through studies of:

- temperature, salinity, density and derived physical variables (obtained from 229, 207 and 192 CTD stations respectively, in the three campaigns; XBT probes were also used to improve the resolution of the temperature field);
- current velocity (ADCP measurements were taken during ALT-SYMPLEX 2 and 3 surveys)
- underwater spectral irradiance field at 52 stations by spectral measurements (Licor LI-1800UW and Satlantic OCI200) and by vertical profiles of PAR at 55 stations, in the campaigns of 1996 and 1998);
- spectral absorption of dissolved coloured and particulate matter, and other related optical properties of seawater, as diffuse attenuation and reflectance, as well as *in vivo* fluorescence of phytoplankton;
- distribution of dissolved nutrients (nitrites, nitrates, ammonia, phosphates and silicates) and total nitrogen and phosphorus;
- phytoplankton lipophilic pigments distribution (HPLC and spectrofluorometric analysis);
- composition of phytoplankton populations in their pico, nano and micro planktonic fractions by both microscopic and

- cytofluorometric analysis;
- primary production through ^{14}C assimilation (P vs E curves and *in situ* simulated incubations);
- variable fluorescence induced by Deep Chlorophyll Maximum Uplifting (DCMU) and light saturation, or measured by PAM and pump & probe techniques.

The number and position of the CTD and XBT casts has been decided in order to have a dense sampling in the region of the cold filament and a global coverage over the central and eastern regions of the channel. Infrared satellite images received on board in real time were used to determine the position of the mesoscale structure. Simultaneous measurements have been conducted during the passages of ERS-2 along tracks 043 and 079 and the passages of TOPEX/POSEIDON along track 059. Along the altimetric tracks, hydrographic profiles were taken every 10 miles and XBT were launched between CTD station.

4 PRELIMINARY ANALYSIS OF SATELLITE DATA

4.1 Satellite data processing

During the experiment five different satellite data-sets have been used: AVHRR-2 images and SeaWiFS data acquired by the High Resolution Picture Transmission (HRPT) receiving station of the Istituto di Fisica dell'Atmosfera (IFA) of Rome, Topex/Poseidon altimeter data received from AVISO (AA.VV. AVISO, 1992, 1995) and ERS-1 and ERS-2 altimeter data obtained from the French processing and archiving facility (F-PAF: CERSAT centre). All AVHRR data acquired from April 1995 until the end of the cruise have been processed from the readout HRPT level to level-1B. Atmospheric corrections were applied and SST and Channel 4 were mapped in geographical projection.

The SeaWiFS data for the period of ALT-SYMPLEX-3 have been decrypted and processed from the readout HRPT level to level-1B. Ocean colour and chlorophyll concentration maps were produced. Moreover, in the pre-cruise phase, TOPEX/Poseidon and ERS-1 SLA data processed by ¹⁴ were merged to compute Sea Level Variability (SLV) in the channel of Sicily. Later comparison of the altimeter data with the simultaneous *in situ* measurements collected during ALT/SYMPLEX has been done using TOPEX/Poseidon and ERS-2 altimetric data preliminary processed by the F-PAF.

Standard quality control, validation, correction of altitude with precise orbit and geophysical and instrumental corrections have been applied to T/P and ERS-2. The final product is sea level anomaly (SLA) calculated, after resampling over regular grids, using repeat-track analysis. This means that the analysis of the SLA gives us information only on the variable part of the oceanographic signal. In order to eliminate from the mesoscale signal the steric effects induced by seasonal warming, seasonal variations due to quasi-stationary large scale currents and eventual errors in the correction of the inverse barometer effect, we have subtracted the average anomaly from each passage on every track. An objective analysis technique was then used to filter the data and to eliminate outliers. For a more detailed description of the altimetric data processing and quality control see also

¹⁵

4.2 Pre-cruise satellite data analysis

The satellite thermal imagery represents an important source of synoptic information about the sea surface dynamics. Daily SST maps of the Sicily channel (from April 1995 to May 1996) were produced and analysed in order to establish the seasonal variability of the surface temperature. The main seasonal behaviour of the SST pattern in the Sicily channel resulting from our analysis is in agreement with previous studies based on AVHRR 18 km weekly data for the period 1982-1992 ¹⁶. The analysis reveals the existence of an area of upwelling along the southern Sicilian coast. In summer this phenomenon is characterised by a strong temperature gradient ($> 3\text{ C}$). It has a wide spatial extension and a long duration in time. In winter the upwelling is limited in time and space to episodic events. In the central part of the channel the entering MAW is always recognised and is limited southward by the resident warm water present south of Malta. The front between these two water masses, called Maltese front, is present year round even if its position varies with the seasons.

The higher resolution of our data-set gives the opportunity to get a more detailed description of the mesoscale features connected to the large scale dynamics. Associated to the upwelling front, instabilities, mushroom-like jets and filaments are observed to feed the mesoscale field. In the summer images two main cold water filament-like patches (20-30 km wide) are often present near Mazara del Vallo and Capo Passero, extending sometimes for more than 100 km offshore. During winter the

two filaments are not always visible and they are rarely observed simultaneously. At this fine space resolution the Maltese front appears as a meandering structure from which eddies and filaments originate.

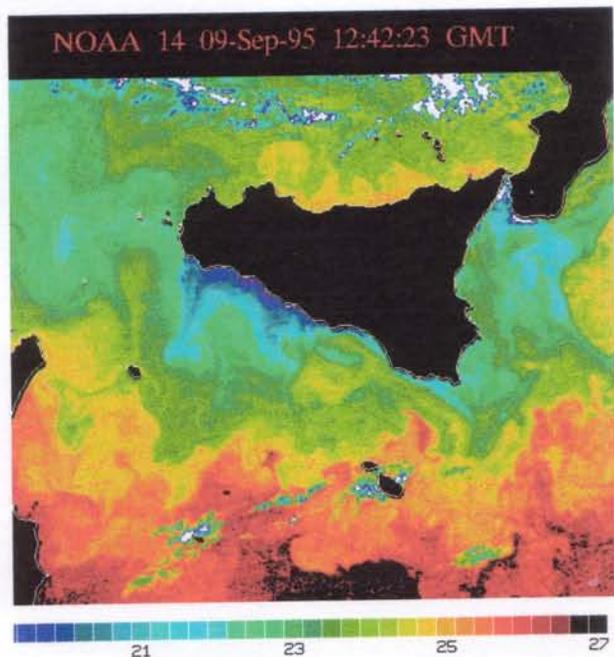


Fig. 2 Summer SST image of the channel of Sicily.

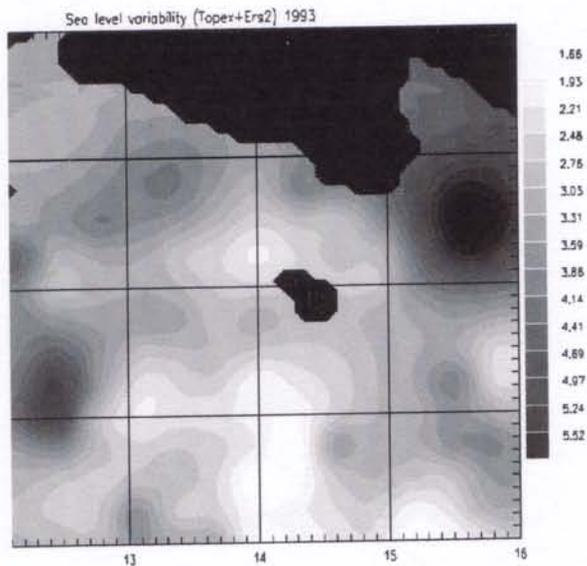


Fig. 3 Sea Level Variability from T/P and ERS-1 (1993)

In figure 2 a typical image of the summer season is presented. An intense coastal upwelling almost fills the northern part of the channel. Two filaments are rooted near Mazara del Vallo and at 37.3°N , 13.5°E . The first one is more elongated, almost reaching Pantelleria island, while the second shows a different aspect ratio. In the area of Capo Passero the upwelled water coastal front detaches from the southern tip of Sicily maintaining its orientation despite the steep deepening of the bottom topography. Instabilities of various length-scales are clearly detected along the Maltese front.

Altimeter data collected during 1993 by ERS-1 and Topex/Poseidon have been used to identify the areas of high surface circulation variability in the Sicily channel. Sea Level Variability maps have been produced from merged data. Figure 3 shows the SLV field for the 1993. The absolute maximum is located 40 km south-east of Capo Passero. It appears as a round structure with a maximum value of about 6 cm, comparable to the most energetic areas in the Mediterranean¹⁷. Connected to this maximum an elongated tongue extends southward 150 km. It reaches the value of 4 cm. These maxima may be related to the variability of the Atlantic-Ionian front and to the recurrence in this area of the filament described previously. Offshore the southern coast of Sicily (at 37°N , 13.5°E), a SLV signal (4 cm) emerges from the weak background field extending for 130-150 km towards the centre of the channel.

Even if the existence of these structures is revealed by SLV calculations relative to one year of data, there is evidence of a strong seasonal variability. During winter (November-May, not shown) the main structure visible in SLV is the maximum south-east of Capo Passero. In summer (June-October, not shown) the pattern is similar to that in figure 4, but here the most energetic area is that where upwelling events are regularly observed.

5

IN SITU DATA ANALYSIS

5.1 General circulation

A synthesis of the effect of the water masses distribution in the area is given by the dynamic heights calculated from hydrologic data (fig.4). We will concentrate on the first and third campaigns. Both surveys were conducted in late winter-early spring and can be easily compared without introducing seasonal variability.

The channel of Sicily is a critical area for the dynamical method. The bottom relief is irregular and often very shallow (fig.1). This means that it is not possible to find any deep no-motion level for the whole area. On the other hand past current meter campaigns (Sparnocchia et al., 1997; Grancini and Michelato, 1987)^{18,7} have confirmed the existence of a zero in the velocity profile at some depth between MAW and LIW. The corresponding surface (identifiable by the salinity gradient maximum) has a very complex structure, causing difficulties in a proper application of the dynamical method. A second choice could be to use as no-motion level the mean depth of the interface between LIW and TIDW (found around 500 m). Dynamic height surface of 300/500 dbar results essentially flat. Consequently we can say that the layer between 300 m and 500 m moves as a whole at the speed found at 500 m. The flow at this depth is known to be very slow and often difficult to detect also with current meters (Grancini and Michelato, 1987)⁷. Therefore the use of 300 m as reference would allow a better coverage without introducing significant errors.

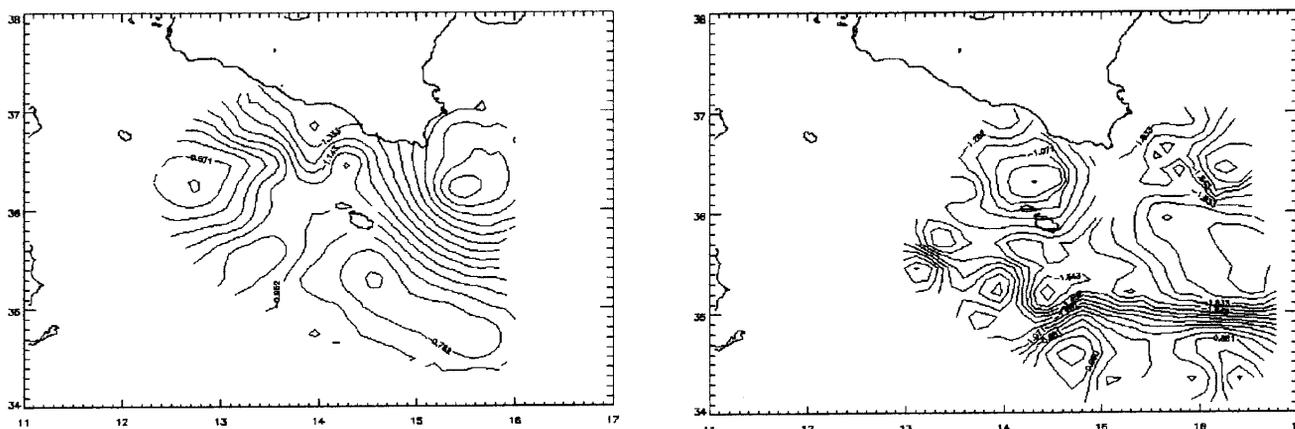


Fig.4 0/300 dbar surfaces from CTD data for the years 1996 and 1998.

Figure 4 shows the dynamic contours of 0/300 dbar surface for 1996 and 1998. In spring 1996 the upper water flows south-east along the Sicily island and splits in two branches in the central part of the channel at 36.3°N, 13.6°E. One branch continues its meandering flow along the Sicilian coast through the Malta channel. Later this water produces a steep front with the Ionian waters (Atlantic-Ionian Front), showing a cyclonic tendency. The other branch deviates offshore, meeting an intrusion of warm and salty water from the region south of Malta.

During ALT-SYMPLEX-98 survey the south eastern area of the channel has been covered more extensively by CTD measurements. The MAW flow occupies the whole channel to Capo Passero. On the other hand, the Atlantic-Ionian front is now oriented south-west. The Ionian waters and the warm resident waters south of 35°N thus constrain the MAW to flow between 35.5°N and 34.8°N at the longitude of Malta. This intense jet is clearly visible in 0/300 dbar surface. The flow presents some meandering inside the channel, while it continues straightforward to the Ionian Sea east of 15°E.

5.2 Composition of phytoplankton assemblages

Preliminary data result from the combination of flow cytometric, HPLC and microscopic analyses. In the spring of 1996 and 1998 coastal waters could be differentiated from offshore ones not only from biomass concentrations, higher at the coast, but also by typical populations of phytoplankton. Infact, diatoms dominated at the coast with the genera *Chaetoceros*, *Pseudonitzschia* and *Thalassionema*. Prymnesiophytes were widespread, and very abundant at some stations. Nanoflagellates belonging to the Prymnesiophytes dominate offshore waters, with the coccolithophore *Emiliania huxleyi* as dominant species. HPLC as well as microscopic data reveal that small dinoflagellates, Cryptophytes and undetermined flagellates belonging to Prasinophytes and Chlorophytes give a significant contribution to total biomass offshore. Picophytoplankton (algae of size less than 2 µm), as revealed by flow cytometry, is characterized by phycoerythrin-containing *Synechococcus* spp., most abundant in surface waters, while *Prochlorococcus marinus* is relatively more abundant at depth. This species dominates the deep fluorescence maxima at offshore stations, as revealed by flow cytometry and *in vivo* spectra of fluorescence and absorption. Deep populations of *P. marinus* are always characterized by a bimodal distribution of scatter and fluorescence, suggesting the existence of two different populations, similar to what found by¹⁹ in the Pacific Ocean.

On the contrary, *P. marinus* abundances increase in the summer, when algae of size less than 2 µm dominate all over the

investigated area. In particular, they are responsible for the deep fluorescence and chlorophyll maximum, together with picoeukaryotes, which often show relative maxima at depth. In the summer of 1997 a filament was present in the area, corresponding to an upwelling of colder and richer water. Such structure was marked by an increase of *P. marinus* cells with an higher fluorescence with respect to populations of nearby stations. Such higher fluorescence suggests that the upward transport was so recent that cells were not allowed yet to photoacclimate and also shows that picoplankton can be used as indicator of physical processes, due to its small size and resilient nature.

5.3 Photosynthetic activity

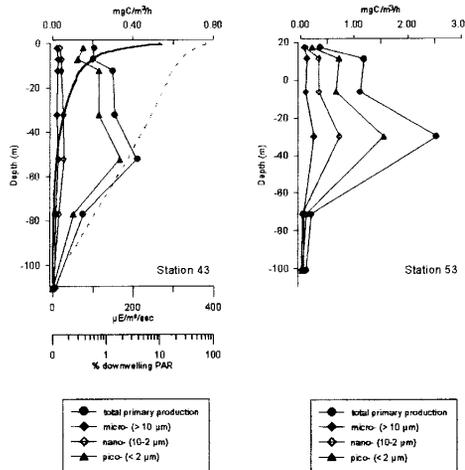


Fig.5 Profiles of primary production for selected Stations in 1996.

C_{14} uptake has been measured in both cruises (1996, 1998). In this section we briefly report on a vertical profile of fractionated primary production measurement in 1996 and on PvsE curves measured during 1998 cruise. Because both cruises have been conducted in the same season and in the same area we consider the results comparable.

In agreement with the dominance of the picoplanktonic part of the community (see above) vertical profiles of fractionated primary production clearly show (fig.5) that the fraction below 0.2 μm is the most active and dominates (around 60%) the photosynthetic activity in the DCM. Picoeukariots which normally occupy the layer just below the DCM do not contribute significantly to water column primary production. In both stations the primary production maximum is located below the first optical depth, but at different depth. This implies a correspondent difference in the light field and yield.

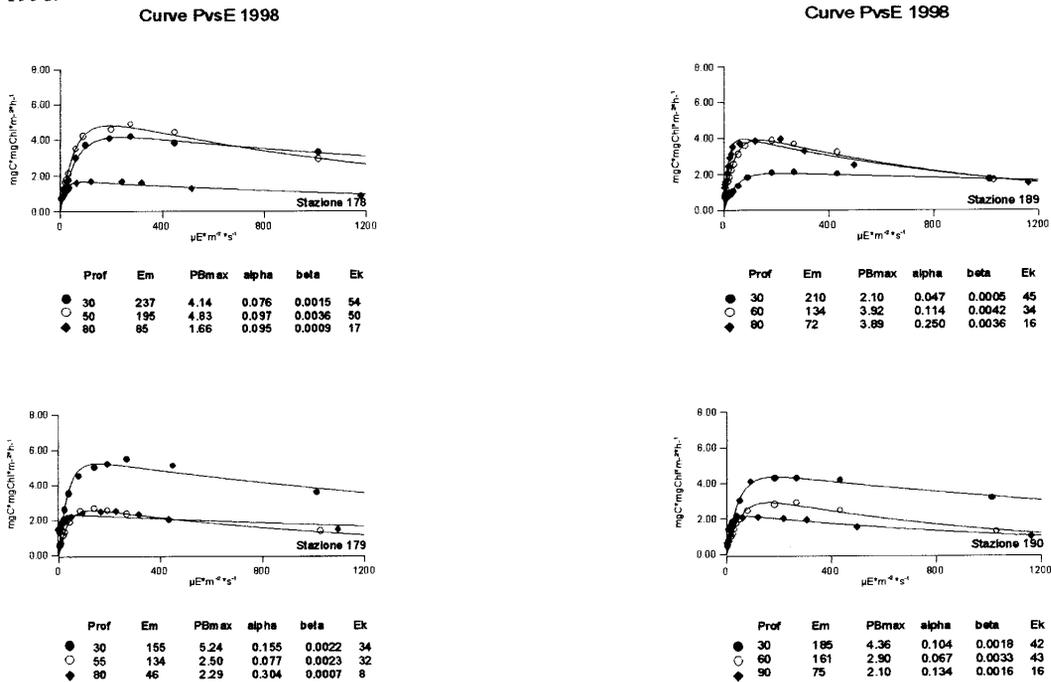


Fig.6 P vs E curves for 1998 on some selected stations.

In 1998 PvsE curves have been obtained for the community in the mixed layer, DCM and below the DCM with the aim of obtaining information on photo-acclimation processes and differences in photosynthetic response along the water column. Fig.6 reports PvsE for two couples of stations sampled at 4 hours time interval at two different sites. All of them are embedded in the cyclonic structure with the first couple (sta. 178-179) being positioned slightly off the centre of it.

Mixed layer community is showing good adaptation at higher light intensity, as to be expected. Likewise the community below the DCM is consistently saturated at the low light intensities of the depth they live in. Less consistent appears the response of the DCM community which alternatively mimic the overlying and underlying community as regards photosynthetic coefficients. The value of PB_{max} is very similar in space and time. This in turn suggests a weak vertical dynamics over the time span of the sampling (36 hours). No data are available for these parameters outside the structure for comparison, but the efficiency and the PB_{max} measured for the mixed and the DCM layer are relatively high. *In situ* irradiance at sampled depths was always below the saturation values, i.e. in the light limitation region of the curve.

5.4 Spectral in situ reflectance and biomass

The most commonly used algorithm to retrieve surface Chlorophyll concentration (C_{pd}) are based upon the reflectance model considering two wavelengths around 440 and 560 nm²⁰. Following this model for the Sicily Channel data, the regression between C_{pd} vs $R(443)/R(560)$ $\log C_{pd} = 0.139 - 1.93 \log R(443)/R(560)$ (with $n=41$, $r=0.89$) (fig.7) shows accordance with literature²⁰.

The accuracy of this model, also in case I waters, is affected by the variability linked to environmental conditions in the reciprocal ratios between phytoplankton, detritus and CDOM absorption²¹, which are the most important factors determining reflectance, together with backward diffusion.

The bio-optical measurements carried out in the Sicily Channel are focused on the separation of the individual contribution of phytoplankton, detritus and CDOM to total absorption to study the relationships between the major absorber at mesoscale, and to produce a local model for retrieval of the phytoplankton biomass. The availability of the 412 nm SeaWifs band will permit to include, at least partially, this variability between the major absorber, reducing the overestimate of the blue absorption of phytoplankton due to detritus and CDOM²².

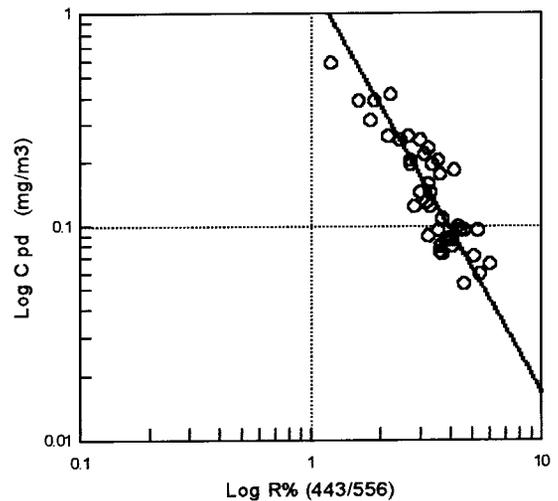


Fig. 7 Orthogonal regression of $\log C_{pd}$ vs $\log (R443/R556)$.

6 MESOSCALE PHENOMENA DURING ALT-SYMPLEX-3

During the second half of the ALT-SYMPLEX-3 survey, 4 days (12-16 April 1998) have been devoted to the monitoring at a high spatial resolution of the region east of Capo Passero. The thermal images received on board at that time showed a system of small eddies advecting nutrient-rich water from the coastal areas. In the following we present a preliminary analysis of the data collected, both from a physical, biological and bio-optical point of view.

6.1 Hydrographic fields and ADCP measurements

The structure studied consists of two small eddies centered at 36.65°N-15.65°E (anti-cyclon) and 36.4°N-15.8°E (cyclon) respectively. These two eddies are visible in the surface velocity field (24m) reconstructed from the ADCP data (fig.7). The anti-cyclon originates from a tongue of cooler and less saline water ($S \sim 37.9$, fig.8) well identifiable as an intense jet (> 35 cm/s) of coastal water in the western part of the sampled area. This water is wrapping with the saltier water from east ($S \sim 38.1$) in the cyclonic structure. These small mesoscale features were monitored while developing, as satellite imagery showed a very rapid growth and evolution during the 4 days. A complete dynamical analysis is in progress.

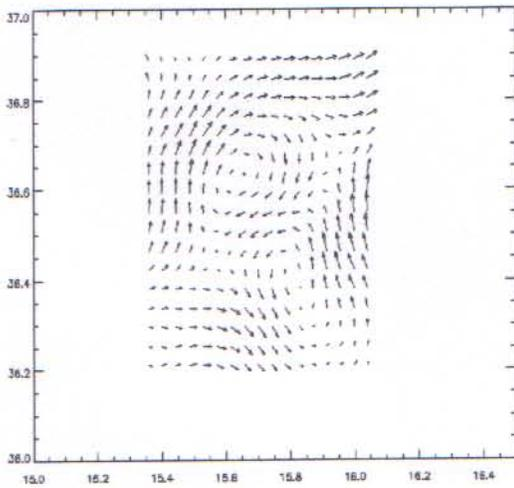


Fig.8 Surface velocity field from ADCP data.

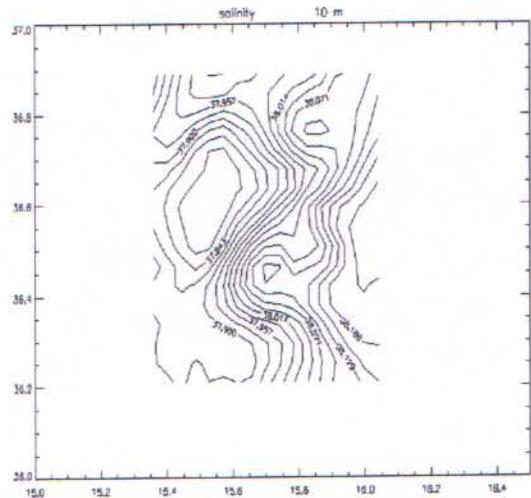


Fig.9 Map of salinity at 10 m.

6.2 Chlorophyll *a* distribution

Chlorophyll *a* fields for 1998 cruise have been reconstructed by a fit of *in situ* fluorometric profiles with data from acetone extracts of chlorophyll of Niskin samples using a neural network algorithm¹⁸. This allowed a higher data resolution for the gridding routine to derive the horizontal maps. Depth of the euphotic zone and of the first optical depth have been estimated for each station by an empirical log-log fit of depth integrated chlorophyll *a* values and downwelling PAR profiles at the stations where both data were available. From those, two maps have been generated for the first optical depth (SeaWiFS detectable layer) and for the underlying layer down to 100 m. The maps are reported in figure 9.

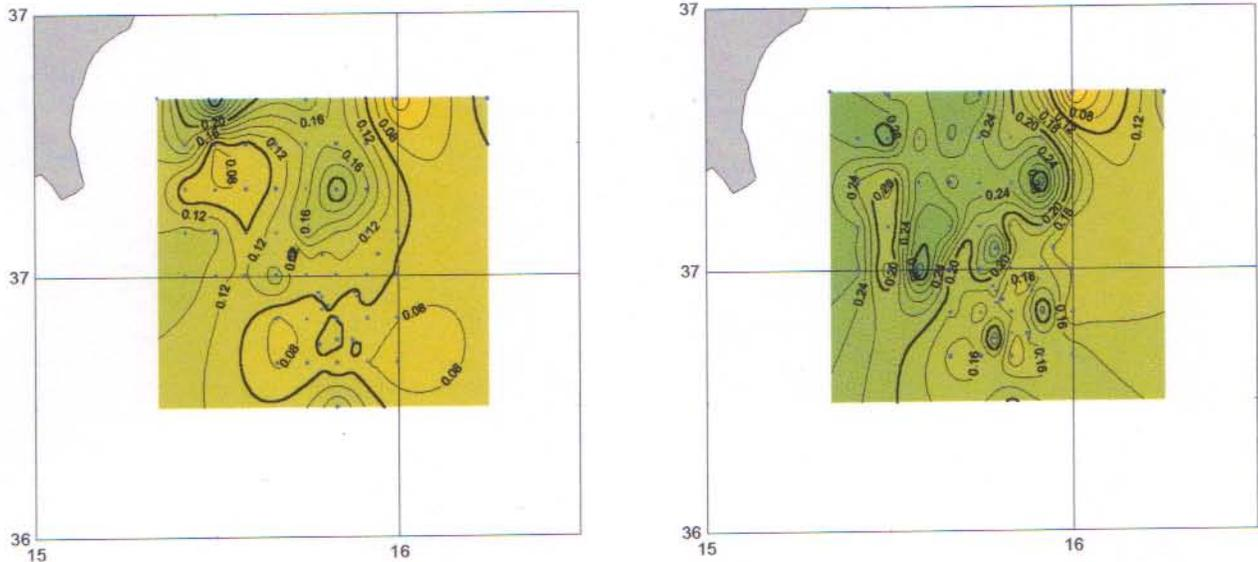


Fig.10 Maps of chlorophyll integrated to the first optical depth and from the first optical depth to 100m.

Phytoplankton biomass, as chlorophyll *a*, were very low in the surface layer (generally below $0.2 \text{ mg}\cdot\text{m}^{-3}$) with minimum at maximum values of 0.06 and $0.28 \text{ mg}\cdot\text{m}^{-3}$, respectively. In the subsurface layer, where the Deep Chlorophyll Maximum was located, depth averaged values are generally 50% higher and display more defined spatial patterns in the range of Mediterranean mesoscale (10-50 km). The analysis of vertical profiles (not shown) does not indicate a significant uplifting in the depth (60 m) of DCM in the cyclonic structure as delimited by dynamic data, whereas in the anticyclonic eddy a more complex, three peaked, fluorescence distribution, suggests a coupled horizontal dynamics.

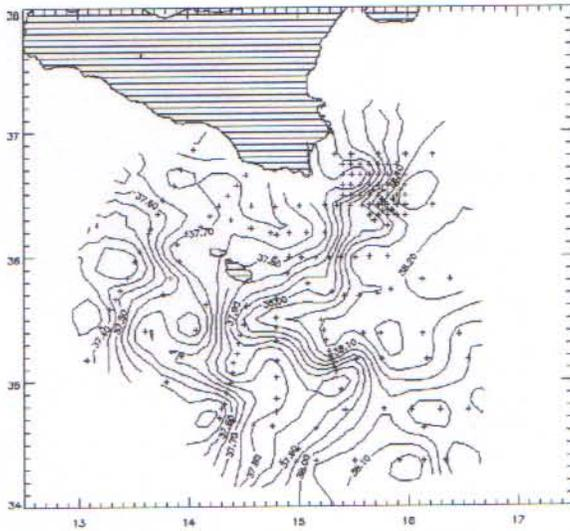


Fig.13 Surface salinity map during ALT-SYMPLEX-3 survey.

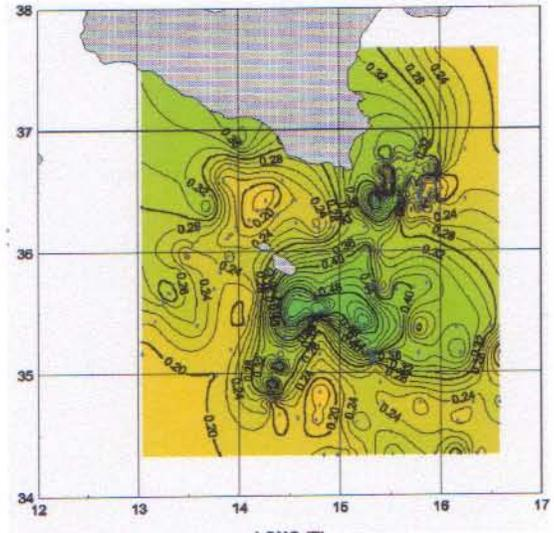


Fig.14 Integrated fluorescence on the layer 0-100m.

7.2 Comparison with in situ data at meso-scale

The high spatial resolution of both biological and physical fields in the area east of Capo Passero permits to investigate more accurately the correspondence between satellite data and in situ measurements also in presence of a strong mesoscale activity. In figure 14 the contour lines of the measured chlorophyll integrated to the first optical depth (§6.2) have been plotted over the SeaWiFS image of April 14. The two chlorophyll fields appear highly correlated. A filament rich of chlorophyll is identified in the northern part of the area studied, where the highest values are found. This tongue of water is advected by the anti-cyclonic eddy observed, while a minimum in the chlorophyll concentration is found at 36.65°N-15.60°E in both maps.

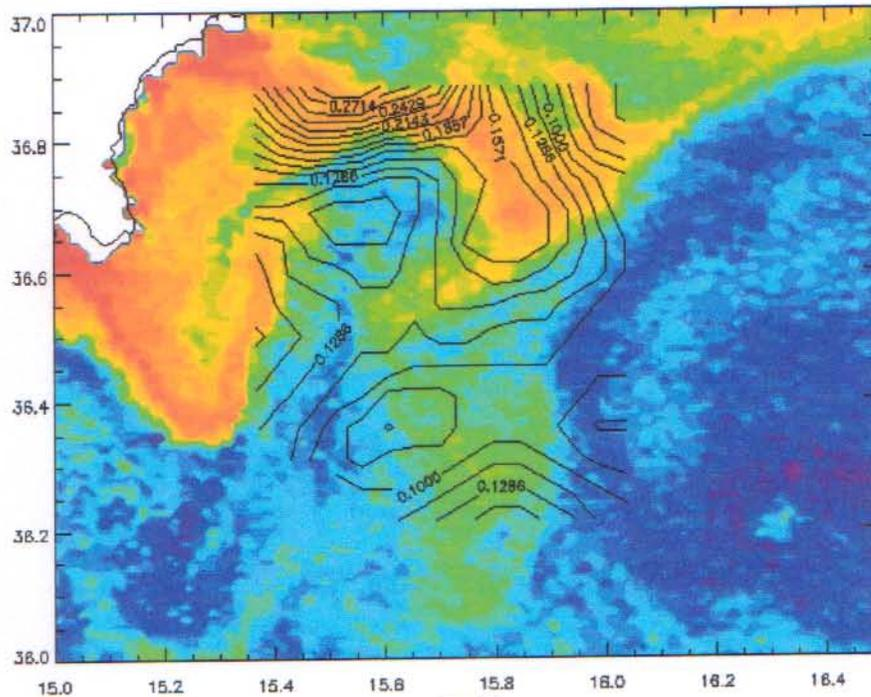


Fig.15

A more quantitative comparison between satellite derived parameters and in situ measurements is underway looking either to the in situ and satellite chlorophyll measurements or to the underwater spectral radiance and SeaWiFS band measurements. Up to date the chlorophyll values obtained from satellite result higher than the measured ones for a factor ~2.

1. Robinson A.R., Golnaraghi M., 1994. Physical and dynamical oceanography of the Mediterranean Sea, in *Ocean Processes in climate dynamics: global and Mediterranean examples*, ed. by Malanotte-Rizzoli e A.R. Robinson, NATO ASI Series, Vol.4, 19, 225-306.
2. Falkowski, P. G., D. Ziemann, et al. (1991). "Role of eddy pumping in enhancing primary production in the ocean." *Nature* 352: 55-58.
3. McGillicuddy, D. J., A. Robinson, R., et al. (1998). "Influence of mesoscale eddies on new production in the Sargasso Sea." *Nature* 394: 263-266.
4. Oschlies, A. and V. Garçon (1998). "Eddy-induced enhancement of primary production in a model of the North Atlantic Ocean." *Nature* 394: 266-269.
5. Garret C.J.R., 1983. Variable sea level and strait flows in the Mediterranean: a theoretical study of the response to meteorological forcing. *Oceanol. Acta*, 6, 1, 79-87.
6. Ozturgut E., 1978. Temporal and spatial variability of water masses: the Strait of Sicily (MEDMILOC 72), SACLANT CEN SM-65, La Spezia, Italy, SACLANT ASW Research Centre.
7. Grancini G. F., Michelato A., 1987. Current structure and variability in the Strait of Sicily and adjacent area, *Annales Geophysicae*, 5B, (1), 75-88
8. Manzella G. M. R., Gasparini G. P. & Astraldi M., 1988. Water exchange between the eastern and western Mediterranean through the Strait of Sicily. *Deep Sea Res.*, 35, 6, 1021-1035.
9. Manzella G. M. R., 1994. The seasonal variability of the water masses and transport through the Strait of Sicily, in *The seasonal and interannual variability of the western Mediterranean Sea*, ed. by P.E. LaViolette, Series on Coastal and Estuarine Studies, American Geophys. Union, Vol. 46, 33-45.
10. Manzella G.M.R., Hopkins T.S., Minnet P.J., Nacini E., 1990. Atlantic water in the strait of Sicily, *J. of Geophys. Res.*, 95, 1569-1575.
11. Morel A., 1972. The hydrographic characteristics of the water exchanged between the eastern and the western basins of the Mediterranean. In *Oceanography of the Strait of Sicily*, SACLANTCEN Conf. Proc. 7, La Spezia, 11-37.
12. Moretti M., Sansone E., Spezie G., De Maio A., 1993. Results of investigations in the Sicily channel, *Deep sea res.*, II, vol. 40, 6, 1181-1192.
13. Astraldi M., Gasparini G.P., Sparnocchia S., Moretti M., Sansone E., 1996. The characteristics of the water masses and water transport in the Sicily strait at long time scales. *Bulletin de l' institut oceanographique*, Monaco, 17th CIESM Science series n° 2.
14. Zoffoli S., Santoleri R., Marullo S., Buongiorno Nardelli B., 1997. The contribution of Topex/Poseidon and ERS-1 altimeter data to investigate the seasonal variability of mesoscale structures in the Mediterranean sea. Submitted to *International Journal of Remote Sensing*.
15. Iudicone D., Marullo S., Santoleri R., Gerosa P., 1998. Sea level variability and surface eddy statistics in the Mediterranean sea from Topex/Poseidon data, accepted *J. of Geophys. Res.*
16. Marullo S., Santoleri R., Malanotte Rizzoli P., Bergamasco A., 1998. The sea surface temperature field in the eastern Mediterranean from AVHRR data. Part I. Seasonal variability, *J. Marine System*, In press.
17. Larnicol G., Le Traon P.Y., Ayoub N., De Mey P., 1995. Mean sea level and surface circulation variability of the Mediterranean Sea from 2 years of TOPEX/POSEIDON altimetry, *J. Geophys. Res.*, C12, 163-177.
18. Scardi M. (1996) "Artificial neural networks as empirical models for estimating phytoplankton production" *Mar. Ecol. Progr. Ser.* 139: 289-299
19. Campbell L and Vaultot D., 1993. Photosynthetic picoplankton community structure in the subtropical North Pacific Ocean near Hawaii (station ALOHA). *Deep-Sea Res. I* 40(10): 2 043-2060.
20. Massi L. , Biondi N., Lazzara L., Innamorati M. (in preparation) Phytoplankton, detritus and CDOM absorption relationships with phytoplankton biomass in oligo- and mesotrophic case I waters .
21. Carder K.L., Hawes S.K., Baker K. A. , Smith C. S. , Steward R.G., and Mitchell B. G. 1991 Reflectance model for quantifying chlorophyll a in the presence of productivity degradation products, *J. Geophys. Res.*, 96 (c11), 20599-20611